



Title	Unsteady Separated Flow behind a Normal Plate Calculated by a Discrete-Vortex Model : Part 2. Modification of Velocity-Point Scheme
Author(s)	Kiya, Masaru; Arie, Mikio; Harigane, Katsuyuki
Citation	Memoirs of the Faculty of Engineering, Hokkaido University, 15(2), 211-222
Issue Date	1979-12
Doc URL	http://hdl.handle.net/2115/37985
Type	bulletin (article)
File Information	15(2)_211-222.pdf



[Instructions for use](#)

Unsteady Separated Flow behind a Normal Plate Calculated by a Discrete-Vortex Model

(Part 2. Modification of Velocity-Point Scheme)

Masaru KIYA* Mikio ARIE* Katsuyuki HARIGANE*

(Received June 30, 1979)

Abstract

The reduction in the strength of the vortices as a function of their age is introduced to represent the cancellation of vorticity in the formation region of the rolled-up vortices. It is found that this modified version of the discrete-vortex model predicts the drag force, the rate of shedding of vorticity from the separation points and the convection velocity of the rolled-up vortices in much more satisfactory manner than the original model developed in Part 1. The time-averaged velocity and root-mean-square values of the fluctuating velocity components in the near wake showed fairly good agreement with a careful measurement by Bradbury (1976). The accuracies of these predictions are indeed comparable to those of the results obtained by means of the sophisticated turbulence-model equations (Pope & Whitelaw 1976). An unfavourable aspect of the reduction in the strength of the vortices is an increase in the Strouhal number, the calculated value of the Strouhal number being larger by 33 percent than experiments.

1. Introduction

From the results described in Part 1 [1], it becomes clear that some modifications of the velocity-point scheme will be necessitated in order to obtain a satisfactory prediction of the time-averaged velocity and fluctuating properties of the near wake behind the plate. The authors believe that the absence of sufficient cancellation of vorticity in the formation region is one of the most serious shortcomings of the discrete-vortex approximation in general when it is applied to the separated flows past bluff bodies.

The cancellation of vorticity mostly caused by a number of elemental vortices entering a vortex cluster of opposite sign amounts only to 10 percent at most, which is much smaller than the value 34~70 percent observed experimentally. Therefore, one must introduce some artificial procedures to promote the mixing of elemental vortices of opposite sign or reduce their strength as a certain function of time. These procedures are attempts to incorporate into the discrete-vortex model the viscous and/or turbulent diffusion of vorticity. The enhanced mixing of vortices may be realized by superposing on the motion of vortices the random walks of an appropriate variance and zero mean, which can be effected by generat-

*) Fluid Mechanics I, Department of Mechanical Engineering.

ing Gaussianly distributed random numbers in a computer. The variance of the random walks will be determined on the basis of the viscous and/or turbulent diffusion coefficient of vorticity in actual wakes. This procedure was actually tested at a preliminary stage of the present investigation. Although the random walks did promote the mixing of vortices, however, they were unable to bring about the amount of cancellation of vorticity comparable to that observed experimentally without suppressing the definite periodic vortex shedding from the plate. Insufficient variance of the random walks led to no significant improvements of the predicted results compared with the case of no random walks.

Moreover, it was found that an increase in the variance of the random walks was qualitatively accompanied by the change of aerodynamic characteristics of the plate corresponding to an increase in the decay rate of the strength of elemental vortices. Since, as will be seen later, the reduction in the strength of the vortices makes fairly good predictions of the wake characteristics, the introduction of the random walks has been abandoned and hence the following discussions will be restricted to the former case. The definition of symbols is the same as in Part 1, unless otherwise stated.

2. Modification of Velocity-Point Scheme

It was assumed that the strength of elemental vortices was reduced according to the law

$$\Gamma(t)/\Gamma_0 = 1 - \exp\left(-\frac{\sigma^2}{4\nu t}\right) \quad (1)$$

where Γ_0 is the initial strength of vortices, $\Gamma(t)$ their strength at time t (age of the vortices) and σ denotes the cut-off radius of the vortices. This decay law was adopted because it is the solution of Navier-Stokes equations for an isolated rectangular viscous vortex initially concentrated on the axis of rotation provided that σ is replaced by the radial distance r from the center of the vortices. Introducing the non-dimensional variable and parameters defined by $\tilde{t} = U_\infty t / (2a)$, $\tilde{\sigma} = \sigma / (2a)$ and $Re = U_\infty (2a) / \nu$ (Reynolds number), the argument of the exponential function, i. e. $\sigma^2 / (4\nu t)$, is written as $\tilde{\sigma}^2 Re / (4\tilde{t})$. Accordingly, since the initial strength Γ_0 is determined from the velocity at the velocity point, one need only to assign the value of the combination $\tilde{\sigma}^2 Re$ in order to calculate the decay of the strength of the vortices.

Let $2a\tilde{\tau}_K / U_\infty$ denote the period of vortex shedding from one edge of the plate and $2a\delta\tilde{t} / U_\infty$ the time interval between the introduction of new vortices into the wake. Also let the maximum integer not exceeding $\tilde{\tau}_K / \delta\tilde{t}$ be denoted by N . Then the total strength Γ_t of the vortices included in a vortex cluster is written as

$$\Gamma_t = \sum_{j=1}^N \Gamma_j \left[1 - \exp\left(-\frac{\tilde{\sigma}^2 Re}{4j\delta\tilde{t}}\right) \right] \quad (2)$$

where Γ_j is the initial strength of the j -th elemental vortex. For the sake of simpli-

city, one approximates Γ_j by an arithmetic average $\Gamma_m = N^{-1} \sum_{j=1}^N \Gamma_j$, the total strength being equal to $N\Gamma_m$. If it is assumed that the fraction $(1-\lambda)$ of the total vorticity is cancelled in the formation region, one obtains

$$\lambda N = \sum_{j=1}^N \left[1 - \exp\left(-\frac{\bar{\sigma}^2 Re}{4j\delta\bar{t}}\right) \right] \quad (3)$$

Accordingly, if the value λ is assigned on the basis of experimental information, equation (3) can be solved to yield an appropriate value of the parameter $\bar{\sigma}^2 Re$.

In the following calculations, the distance between the velocity points and the edges of the plate is selected to be $\delta/(2a)=0.1$. Since the Strouhal number St for a normal plate is about 0.15 on the average, the values of $\bar{\tau}_K$ and N become $\bar{\tau}_K = 2/St = 13.3$ and $N = [\bar{\tau}_K/\delta\bar{t}] = 41$ because $\delta\bar{t} = 0.32$. The values of the other parameters are the same as those employed in Part 1.

Previous experimental investigators suggested that the value of λ fell between 0.34 and 0.70. If $\lambda=0.6$ is employed as a typical value, which yields $\bar{\sigma}^2 Re = 20$, the temporal variations of $\partial\Gamma/\partial t$ and C_D become as shown in Fig. 1. No sign of periodic vortex shedding is observed in the curves of $\partial\Gamma/\partial t$ and C_D , together with the vortex patterns in the wake which are not presented here. The time-averaged values of $\partial\Gamma/\partial t$ and C_D are 1.1 and 2.08 respectively and higher by 6 and 12 percent than the experiment. However, time-averaged velocity in the wake was found to be much larger and, on the contrary, the root-mean-square values of the fluctuating velocities were much less than the experiment. This feature was undoubtedly brought about by an unreasonably large reduction in the strength of the vortex clusters immediately behind the plate. Thus one is led to the conclusion that the value of $\lambda=0.6$ is too small to yield the prediction of the near-wake characteristics consistent with the experiment.

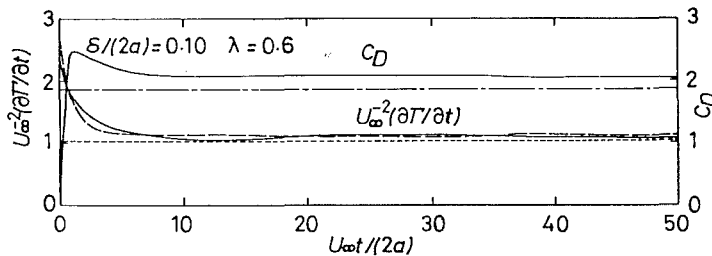


Fig. 1. Temporal variations of C_D and $U_\infty^2(\partial\Gamma/\partial t)$ for $\lambda=0.6$.

An optimum value of $\lambda=0.8$ was found after some trial and error, $\bar{\sigma}^2 Re$ being found to be 40. The wave forms of $\partial\Gamma/\partial t$ and C_D obtained for this case are shown in Fig. 2. Periodic vortex shedding is evident particularly in the wave form of $\partial\Gamma/\partial t$. Most noteworthy in these curves may be the rather rapid increase in C_D and amplitude of $\partial\Gamma/\partial t$ after the time in the neighbourhood of $U_\infty t/(2a)=50$ is passed. If the integration between $U_\infty t/(2a)=25.92$ and 44.8, during which two cycles of vortex shedding have occurred and there have been at least four vortex

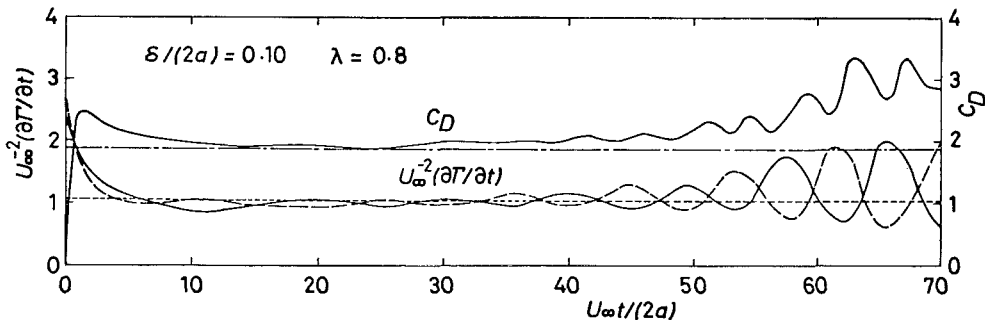


Fig. 2. Temporal variations of C_D and $U_\infty^{-2}(\partial\Gamma/\partial t)$ for $\lambda=0.8$.

clusters behind the plate, is employed to calculate the time-averaged values of $\partial\Gamma/\partial t$ and C_D , one obtains $\overline{\partial\Gamma/\partial t}=1.07$ and $\overline{C_D}=2.0$. These values are larger by 3 and 8 percent at the most than the measurement of Fage and Johansen [2] corrected for the wind-tunnel blockage effect. These errors are believed to be among the smallest of the discrete-vortex calculations of the separated flows past inclined flat plates (Kuwahara [3], Sarpkaya [4] and Kiya and Arie [5]). Much larger $\overline{\partial\Gamma/\partial t}$ and $\overline{C_D}$ will be obtained if, for instance, the integration over the time interval $U_\infty t/(2a)=60\sim 70$ is employed. For later convenience, the state of flow prevailing during the two representative time intervals, i. e. $U_\infty t/(2a)=25.92\sim 44.8$ and $U_\infty t/(2a)\geq 60$ will be designated as state I and state II respectively.

The vortex distributions in the wake at the times $U_\infty t/(2a)=35.2$ and 71.36 , which belong to state I and state II and also correspond to nearly the same phase of the vortex shedding, are shown in Fig. 3. It is clear that the main difference

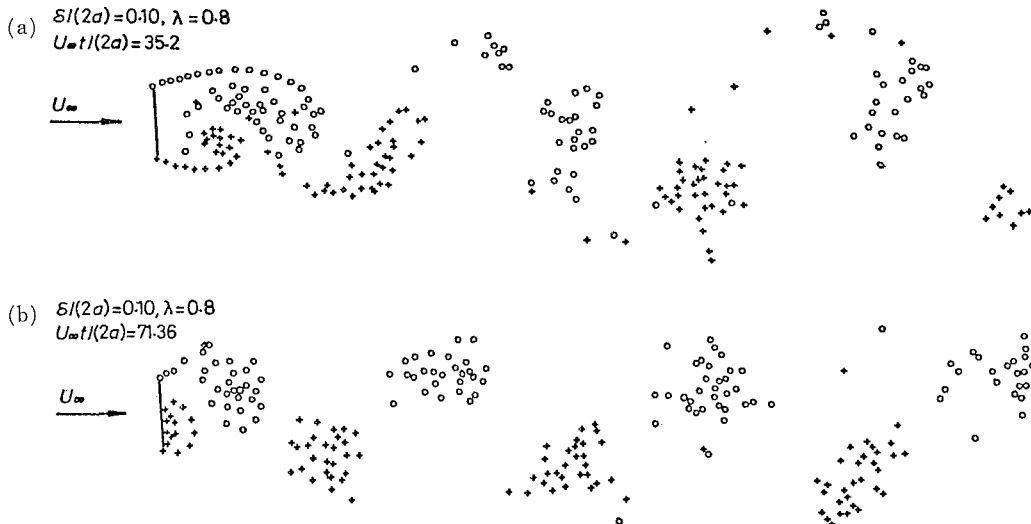


Fig. 3. Vortex patterns in the wake of flat plate of 85° incidence at approximately same phase of periodic vortex shedding.
 (a) $U_\infty t/(2a)=35.2$ (state I), (b) $U_\infty t/(2a)=71.36$ (state II).

between the two vortex patterns is observed in the immediate vicinity of the plate. Namely, in state I, the separated shear layers represented by arrays of point vortices extend farther downstream than those in state II, thus yielding greater length of the formation region of the rolled-up vortices.

Provided that the end of the formation region is defined as the point at which a contour enclosing a growing vortex cluster crosses the center of the wake at the instant the vortex cluster leaves the plate, the length of the formation region is approximately 2.25 (state I) and 1.45 (state II) times the height of the plate. Since experimental studies sufficiently detailed to permit the determination of the formation length behind a normal plate are not known to the authors, an exact comparison between calculation and experiment is not possible.

Plausible reasons why the transition from state I to state II occurs are not clear to the authors. However, a few additional calculations showed that state II was more stable in the sense that, once state II was established, state I was never recovered.

The Strouhal number determined from the wave form of $\partial I/\partial t$ is approximately 0.20 in state I and 0.25 in state II. Since the velocity-point scheme without the reduction in the strength of the vortices yielded the value of Strouhal number compared well with experiment, this is an unfavourable aspect of the vortex-strength reduction. At the outset the Strouhal number was assumed to be 0.15 in the determination of the parameter $\bar{\sigma}^2 Re$ corresponding to $\lambda=0.8$. Accordingly, in view of the higher Strouhal numbers obtained here, the ratio of the vorticity produced at the separation points to that which is included in the rolled up vortices immediately behind the plate will not equal to 0.8. Actual calculations showed that the ratio was, on the average, 0.72 in state I and 0.85 in state II respectively. In the present calculation the strength of point vortices continues to decrease after the vortex clusters in which they are included have left the formation region. The fraction of the circulation remaining in the vortex clusters in state I amounts to 36 percent on the average when they are in the region $x/(2a)=10\sim 15$ downstream of the plate. Most experimenters employed the data of velocity fluctuations in the region corresponding to $x/(2a)=10\sim 16$ together with particular vortex-street models in order to estimate the value of the fraction, which was shown to be very dependent on the models employed (Davies [6]). Since the values of the fraction thus estimated are 0.6 (Fage and Johansen [2]), 0.43 (Roshko [7]), 0.30 (Bloor and Gerrard [8]) and 0.26 (Davies [6]), the present result may be considered to be reasonable.

The variations of the time-averaged velocity and root-mean-square values of the fluctuating velocities along the center of the wake are shown in Fig. 4. Much improved results of the present calculation are evident if a comparison is made between Fig. 7 of Part 1 and Fig. 4. Although the calculated values of the time-averaged velocity are somewhat higher than the experiment of Bradbury [9], the general trend of the calculated curve is consistent with the experimental one. It may be noted that the accuracy of the present calculation is comparable to that

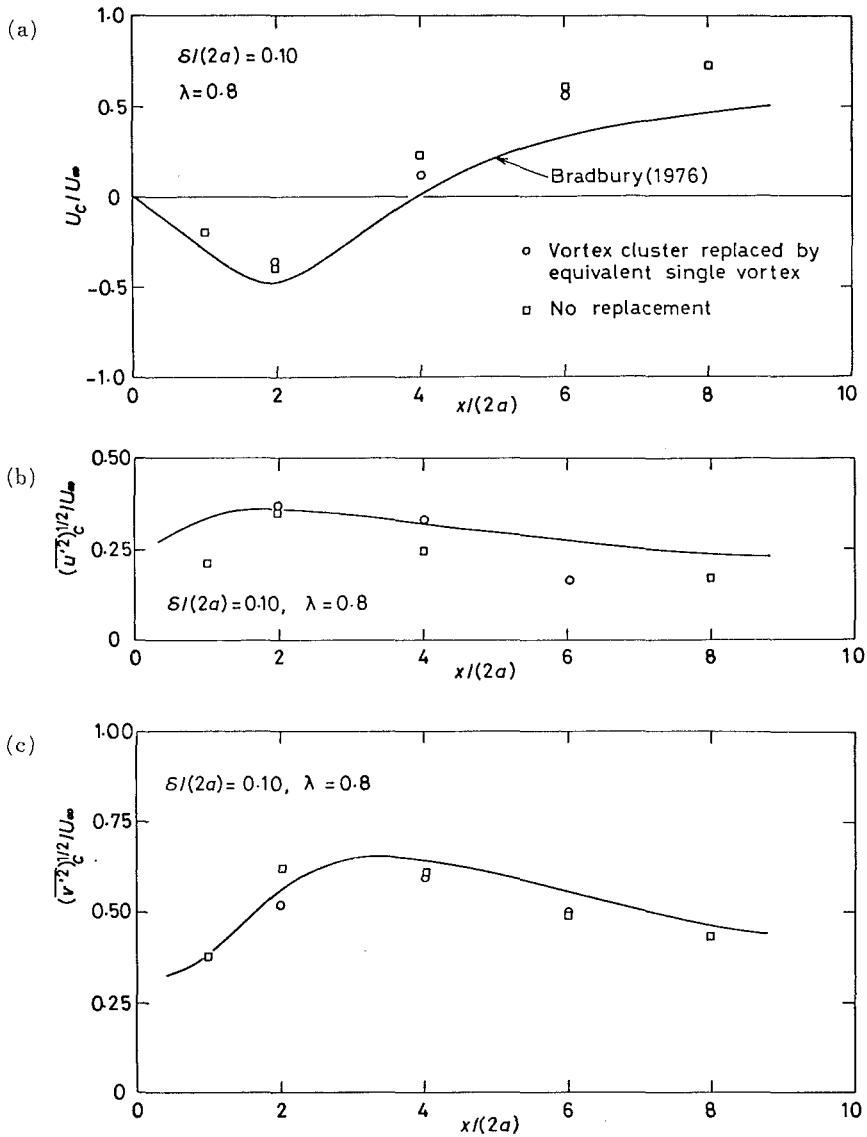


Fig. 4. Variations of time-averaged longitudinal velocity component and root-mean-square values of fluctuating velocity components along the center of wake. State I.

(a) U_c/U_∞ , (b) $(\overline{u'^2})^{1/2}/U_\infty$, (c) $(\overline{v'^2})^{1/2}/U_\infty$.

of the more sophisticated calculation by Pope and Whitelaw [10] who employed the turbulence-model equations to predict the near wake with recirculation behind a circular disc. The distributions of $(\overline{u'^2})^{1/2}/U_\infty$ and $(\overline{v'^2})^{1/2}/U_\infty$ are found to be predicted fairly well, very well indeed in the case of $(\overline{v'^2})^{1/2}/U_\infty$.

The profiles of U/U_∞ and $(\overline{u'^2})^{1/2}/U_\infty$ plotted against $y/(2a)$ are shown in Figs. 5 and 6 together with the experimental results. General agreement between calcula-

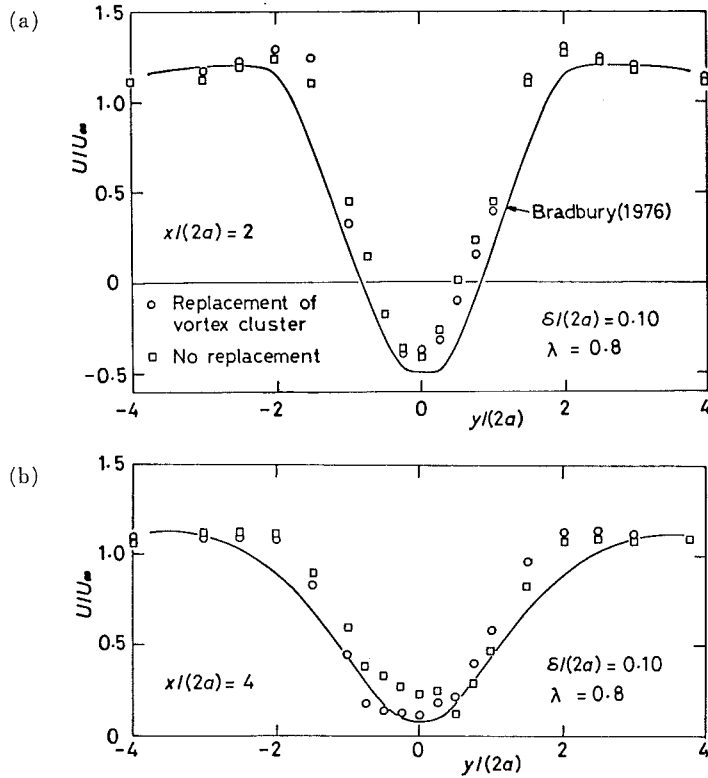


Fig. 5. Distribution of time-averaged longitudinal velocity component in near wake. (a) $x/(2a)=2$, (b) $x/(2a)=4$.

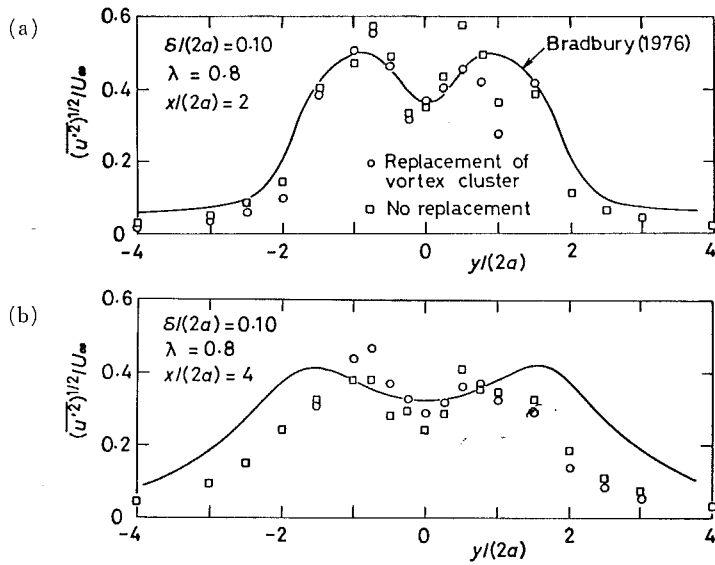


Fig. 6. Distribution of root-mean-square value of fluctuating longitudinal velocity component. (a) $x/(2a)=2$, (b) $x/(2a)=4$.

tion and experiment is fairly good at the stations $x/(2a)=2$ and 4 except that the calculated values of $(\overline{u'^2})^{1/2}/U_\infty$ at the station $x/(2a)=4$ are much smaller in the region $|y/(2a)| \geq 1.5$. A detailed examination of the time-averaged velocity profiles reveals that the predicted width of the wake is somewhat narrower than the experimental one. Moreover, the results presented in Figs. 4~6 demonstrate that the replacement of point vortices in a given vortex cluster by a single vortex has only insignificant effects on the time-averaged and fluctuating properties of the near wake.

The profiles of $(\overline{u'^2})^{1/2}/U_\infty$ and the nondimensional Reynolds shear stress $-\overline{u'v'}/U_\infty^2$ at several downstream distances are shown in Figs. 7 and 8. Since any reliable measurement of these quantities in the near wake of a normal plate is not available to the authors, a detailed comparison between calculation and experiment is not possible. Slight asymmetry observed in the distributions of $(\overline{v'^2})^{1/2}/U_\infty$ and $-\overline{u'v'}/U_\infty^2$ (see Figs. 7 and 8 (b)) may have its origin in the fact that the angle of attack of the plate is not exactly 90° but 85° . Particularly noteworthy may be the very peculiar profiles of the Reynolds shear stress at the stations $x/(2a)=1$ and 2, while the profiles in the more downstream stations are qualitatively consistent with those experimentally observed in the far-wake region. It is hoped that experimental investigations in the near future will clarify the actual distribution of the Reynolds shear stress in the immediate vicinity of the normal plate.

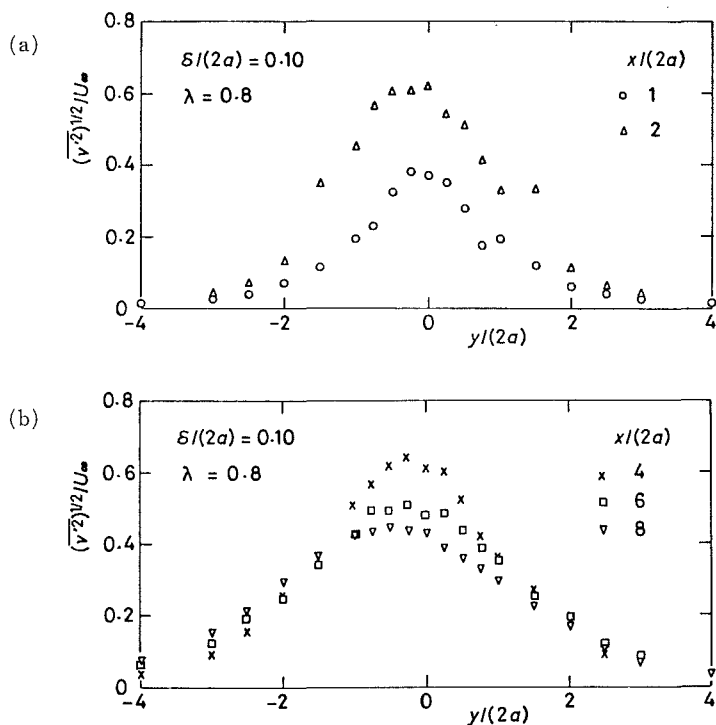


Fig. 7. Distribution of root-mean-square value of fluctuating vertical velocity component in near wake.

(a) $x/(2a)=1$ and 2, (b) $x/(2a)=4, 6$ and 8.

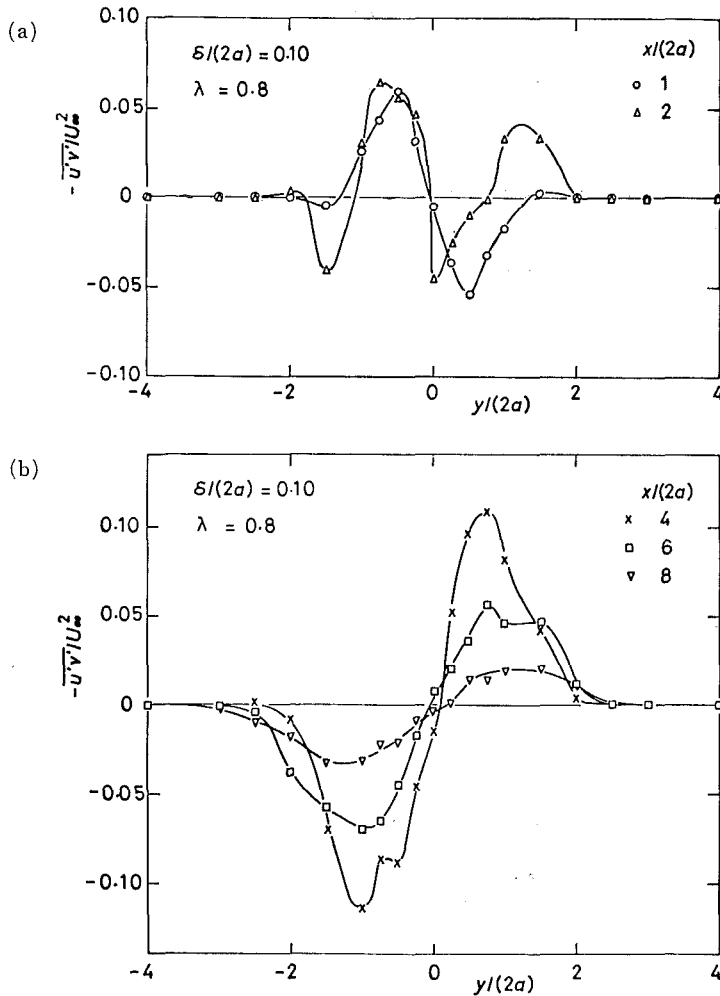


Fig. 8. Distribution of Reynolds shear stress in near wake.
(a) $x/(2a)=1$ and 2, (b) $x/(2a)=4, 6$ and 8.

The convection velocity U_v of the rolled-up vortices is found to slightly increase in the downstream direction. The average value of U_v in the range $x/(2a)=5 \sim 25$, where the measurement of U_v was performed by Fage and Johansen [2], is about $0.88 U_\infty$, which is 13 percent larger than the value $0.766 U_\infty$ obtained by them. In view of the result shown in Fig. 6 of Part 1, it is obvious that the reduction in the strength of vortices increases the convection velocity of the rolled-up vortices.

The results described heretofore might suggest that a value of λ slightly larger than 0.8 will yield better agreement between calculation and experiment with regard to various properties of the separated flow past a normal plate. However, this is not the case. In order to examine the above supposition, additional calculations were performed by setting $\lambda=0.9$. The results showed that state I were almost undetected and state II appeared at about $U_\infty t/(2a)=15.0$ after the start of flow.

The properties of the flow past the plate obtained for this case were almost the same as those described in Part 1.

Finally, the wave forms of the longitudinal and vertical velocity components at several locations in the near wake are shown in Fig. 9, in which approximately two cycles of the vortex shedding are included. Perturbations of higher frequencies, which are the results of nearby point vortices, are superposed on the fundamental periodic wave forms in the central portion of the wake. The general appearance of the wave forms are qualitatively similar to the velocity signals observed experimentally.

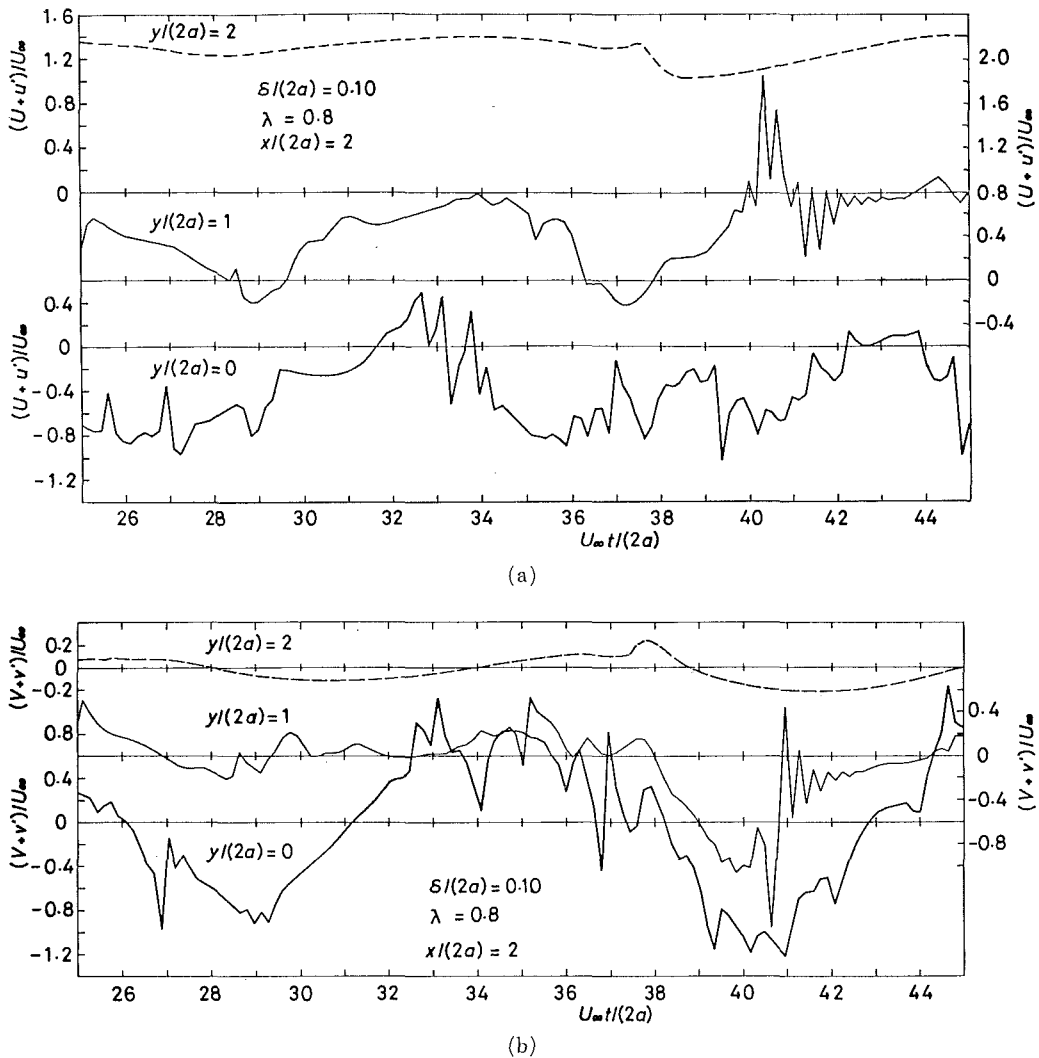


Fig. 9. Wave forms of instantaneous velocity components in near wake at the station $x/(2a) = 2$.

(a) Longitudinal velocity component, (b) Vertical velocity component.

3. Concluding Remarks

The most important finding of the present investigation is that the root-mean-square values of the fluctuating velocity components are fairly well predicted by the discrete-vortex model provided that the reduction in the strength of vortices is appropriately incorporated into the model.

This result is important because the accuracy of the present calculation is almost comparable to that obtained by the use of the sophisticated turbulence-model equations (Pope and Whitelaw [10]). Within the authors' knowledge, previous investigators of the discrete-vortex model failed to examine the properties of the fluctuating velocity components within the near wakes. Accordingly, it seems that the discrete-vortex model, if properly developed further, will emerge as one of the most powerful tools in establishing a link between the characteristics of the wake, the body shape and the resulting forces with relatively few disposable parameters. No other analytical or numerical model has yet been able to produce equally satisfactory results at sufficiently large Reynolds numbers.

At this stage it may be noted that certain important elements in real turbulence are not represented by the discrete-vortex model owing to the absence of viscosity and two-dimensionality of the model. There is no diffusion of vorticity, and hence entrained irrotational fluid remains irrotational, areas of potential flow existing in the simulated turbulent near wake fields where they are known to be impossible. The model contained no streamwise component of vorticity, which is an important constituent of real turbulence. However, despite these shortcomings, many aspects of the large eddy motion which determines the time-averaged flow and main part of fluctuating energies in the near wake are correctly simulated by the present discrete-vortex model.

Some of the further problems to be tackled to improve the present model will briefly be mentioned. Firstly, in order to avoid the complexity to determine the value of δ by trial-and-error method, the location of the velocity points must be assigned on the basis of the boundary-layer characteristics in the vicinity of the separation points of the body. The velocity points should also be allowed to vary as functions of time corresponding to various phases of the vortex shedding from the body. Secondly, in the case of smooth bluff bodies such as a circular cylinder, the Kutta condition which has been used to determine the location of the vortices newly introduced into the wake, must be modified appropriately. Finally the law of the reduction in the strength of vortices should be further examined and developed. It is hoped that an improved version of the present model will yield better predictions of the characteristics of the separated flows past bluff bodies of various shapes.

Reference

- 1) Kiya, M., Arie, M. and Harigane, K.: "Unsteady Separated Flow behind a Normal Plate Calculated by Discrete-Vortex Model. Part 1, Velocity-Point Scheme,"

- Memoirs of the Faculty of Engineering, Hokkaido University, Vol. 15, No. 2, 1979, pp. 199-210.
- 2) Fage, A. and Johansen, F. C.: "On the Flow of Air behind an Inclined Flat Plate of Infinite Span," Proc. Roy. Soc. Lond., Ser. A, Vol. 116, No. 773, 1927, pp. 170-197.
 - 3) Kuwahara, K.: "Numerical Study of Flow past an Inclined Flat Plate by an Inviscid Model," J. Phys. Soc. Japan, Vol. 35, No. 5, 1973, pp. 1545-1551.
 - 4) Sarpkaya, T.: "An Inviscid Model of Two-Dimensional Vortex Shedding for Transient and Asymptotically Steady Separated Flow over an Inclined Flat Plate," Journal of Fluid Mechanics, Vol. 57, Pt. 1, 1975, pp. 109-128.
 - 5) Kiya, M. and Arie, M.: "A Contribution to an Inviscid Vortex-Shedding Model for an Inclined Flat Plate in Uniform Flow," Journal of Fluid Mechanics, Vol. 82, Pt. 2, 1977, pp. 241-253.
 - 6) Davies, M. E.: "A Comparison of the Wake Structure of a Stationary and Oscillating Bluff Body, Using a Conditional Averaging Technique," Journal of Fluid Mechanics, Vol. 75, Pt. 2, 1976, pp. 209-231.
 - 7) Roshko, A.: "On the Drag and Shedding Frequency of Two-Dimensional Bluff Bodies," NACA Tech. Note, No. 3169, 1954.
 - 8) Bloor, M. S. and Gerrard, J. M.: "Measurements of Turbulent Vortices in a Cylinder Wake," Proc. Roy. Soc. Lond., Ser. A, Vol. 294, No. 1438, 1966, pp. 319-342.
 - 9) Bradbury, L. J. S.: "Measurements with a Pulsed-Wire and a Hot-Wire Anemometer in the Highly Turbulent Wake of a Normal Flat Plate," Journal of Fluid Mechanics, Vol. 77, Pt. 3, 1976, pp. 473-497.
 - 10) Pope, S. B. and Whitelaw, J. H.: "The Calculation of Near-Wake Flows," Journal of Fluid Mechanics, Vol. 73, Pt. 1, 1976, pp. 9-32.